

# Estimating the covariance structure of heterogeneous SIS epidemics on networks

E. Cator\*, H. Don† and P. Van Mieghem‡

21 July 2017

## Abstract

Heterogeneous Markovian Susceptible-Infected-Susceptible (SIS) epidemics with a general infection rate matrix  $\tilde{A}$  are considered. Using a non-negative matrix factorization to approximate  $\tilde{A}$ , we are able to identify when a metastable state can be expected, and that the metastable distribution, under certain conditions, will feature a normal distribution with known expectation and covariance. Furthermore, we model a heterogeneous Markovian SIS epidemic, that starts with a fraction of initially infected nodes different from that in the metastable state, by approximating its behaviour by a standard linear stochastic differential equation (SDE) in sufficiently high dimensions. By exploiting the knowledge of the covariance matrix from the SDE, we demonstrate significant accuracy improvements over the first-order mean-field approximation NIMFA.

## 1 Introduction

Epidemic processes on a network can model an amazingly large variety of real-world processes [1], such as the spread of a disease, a digital virus, a message in an on-line social network, an emotion, the propagation of a failure or an innovation and other diffusion phenomena on networks. We confine ourselves here to a particularly simple epidemic model, the Markovian SIS epidemic process, that, as earlier [2] argued, “allows for the highest degree of analytic treatment, which is a major motivation for the continued effort towards its satisfactory understanding”. Here and in addition to [2], we justify that quote. Whereas [2] was based on spectral decomposition, here non-negative matrix factorization and clustering leads to yet another powerful new analytic approximation, entirely different from mean-field theory, but with an accuracy comparable to the well-established mean-field models for large networks. Before outlining the idea of this paper, we introduce definitions and notations.

We consider an unweighted, undirected graph  $G$  containing a set  $\mathcal{N}$  of  $n$  nodes (also called vertices) and a set  $\mathcal{L}$  of  $L$  links (or edges). The topology of the graph  $G$  is represented by a symmetric  $n \times n$  adjacency matrix  $A$  with elements  $a_{ij}$ . In an SIS epidemic process [3, 4, 5, 6, 1, 7] on the graph

---

\*Radboud University Nijmegen, Faculty of Science, P.O. Box 9010, 6500 GL Nijmegen, The Netherlands; *email*: E.Cator@science.ru.nl

†Amsterdam Free University, Faculty of Sciences, De Boelelaan 1081, 1081 HV Amsterdam, The Netherlands, *email*: h.don@vu.nl

‡Delft University of Technology, Faculty of EECS, P.O. Box 5031, 2600 GA Delft, The Netherlands; *email*: P.F.A.VanMieghem@tudelft.nl

$G$ , the viral state of a node  $i$  at time  $t$  is specified by a Bernoulli random variable  $X_i(t) \in \{0, 1\}$ :  $X_i(t) = 0$ , when node  $i$  is healthy, but susceptible and  $X_i(t) = 1$ , when node  $i$  is infected at time  $t$ . A node  $i$  at time  $t$  can only be in one of these two states: *infected*, with probability  $\Pr[X_i(t) = 1]$  or *healthy*, but susceptible to the infection, with probability  $\Pr[X_i(t) = 0] = 1 - \Pr[X_i(t) = 1]$ . We assume that the curing process for node  $i$  is a Poisson process with rate  $\delta_i$  and that the infection rate over the directed link  $(i, j)$  is a Poisson process with rate  $\beta_{ij}$ . Only when node  $i$  is infected, it can infect each node  $k$  of its healthy direct neighbors with rate  $\beta_{ik}$ . All Poisson curing and infection processes are independent. This description defines the continuous-time, Markovian *heterogeneous* SIS epidemic process on a graph  $G$ . We do not consider non-Markovian epidemics [8, 9] and assume that the infection characteristics in the graph, i.e. all curing and infection rates, are independent of time.

Exploiting the important property  $E[X_i] = \Pr[X_i = 1]$  of a Bernoulli distribution, which enables to avoid computations with the probability operator in favor of the easier, linear expectation operator, the exact Markovian *heterogeneous* SIS governing equation [10, 11] for the infection probability of node  $i$  is

$$\frac{dE[X_i(t)]}{dt} = E \left[ -\delta_i X_i(t) + (1 - X_i(t)) \sum_{k=1}^n \beta_{ki} a_{ki} X_k(t) \right] \quad (1)$$

When node  $i$  is infected at time  $t$ ,  $X_i(t) = 1$  and only the first term on the right-hand side between the brackets  $[\cdot]$  affects the change in infection probability with time  $\frac{d\Pr[X_i(t)=1]}{dt}$  (left-hand side in (1)). When node  $i$  is healthy,  $X_i(t) = 0$  and only the second term on the right-hand side between the brackets  $[\cdot]$  increases the change in infection probability with time by a rate  $\sum_{k=1}^n \beta_{ki} a_{ki} X_k(t)$  due to all its infected, direct neighbors. We define the nodal curing vector  $\tilde{\delta} = (\delta_1, \delta_2, \dots, \delta_n)$  and the weighted, infection rate adjacency matrix  $\tilde{A}$  with element  $\tilde{a}_{ij} = \beta_{ij} a_{ij}$ , which is not necessarily symmetric. The governing equation (1) can be evolved into a *heterogeneous* SIS Markov chain containing  $2^n$  states [12, 13, 11], and although the Markov equations are linear and determine the joint probability  $\Pr[X_{j_1}(t) = 1, X_{j_2}(t) = 1, \dots, X_{j_k}(t) = 1]$  of each  $k$ -tuple  $(j_1, j_2, \dots, j_k)$  of nodal indices for  $1 \leq k \leq n$ , the solution of a set of  $2^n$  linear equations is unfeasible for network sizes  $n > 20$ . For special types of graphs that feature symmetry, such as the complete graph and the star [14], fortunately, that huge set of  $2^n$  linear equations can be considerably reduced to a linear in  $n$  number of linear equations, that determine the probability that  $k \in \{0, 1, \dots, n\}$  nodes are infected at time  $t$ .

Our new idea here starts from symmetry as in the complete graph with equal infection rates, where nodes are indistinguishable in the metastable state. Szemerédi's regularity lemma, as explained in [15], roughly tells us that any graph can be partitioned into a bounded number of equal subgraphs and the links among those subgraphs are fairly uniformly distributed, like in random graphs. Here, we will combine both concepts: the indistinguishability of the nodes and the inherent, topological partition structure of a graph. First, we approximate the infection rate adjacency matrix  $\tilde{A}$  by invoking non-negative matrix factorization (NMF) [16] as

$$\tilde{A}_{n \times n} \simeq (W^T)_{n \times k} H_{k \times n}$$

where  $W$  and  $H$  are  $k \times n$  matrices, where in general  $k \ll n$ . Earlier in [17], the influence of a community structure on the spread of epidemics was studied. By invoking the concept of equitable partitions and the quotient matrix [18, p. 23-25], Bonaccorsi *et al.* [19] have formalized the observations in [17] to clustering in networks, that exhibit a relatively easily recognizable partitioning (such

as the interconnection of cliques). Based on graph partitioning and the isoperimetric inequality, the universal mean-field framework (UMFF) [20] further generalizes graph partitioning for mean-field epidemics and incorporates a wide variety of different mean-field approximations such as NIMFA [21] and the Heterogeneous Mean-Field (HMF) [22]. We believe that NMF is generally applicable to networks, that do not immediately unveil an obvious partition structure. The second step in our approach is to study the SIS behaviour whenever the infection rate matrix  $\tilde{A}$  is of the form  $W^T H$ . It is well known [23] that NMF can be used to perform a clustering of the  $n$  nodes. This clustering or partitioning idea transforms the SIS epidemics into a solvable stochastic diffusion process, which is amenable not only to the analysis of the quasi-stationary or metastable configuration, but even to the analysis of the time-evolution of the SIS epidemics as shown in Section 4.

Our method, called “clustered SIS”, is evaluated in Section 5 on both a synthetic power law graph as well as on a real-world network, derived from an airport network. Aimed to encompass most mean-field approximations, UMFF [20] only provides general bounds on the accuracy of mean-field approximations derived from the isoperimetric inequality. UMFF does not propose mean-field accuracy improvements techniques, in contrast to this paper. In particular, the estimate of the covariance matrix  $\Sigma_\infty$  in the metastable state, deduced from the stochastic vector differential equation (18) by linearization (Appendix A.1) is given in a closed form expression (24) and its incorporation significantly improves the accuracy of the first-order mean-field approximation NIMFA as demonstrated in Section 5.3 on a real-world network. While earlier no specific information about the correlation structure  $E[X_i X_k]$  between any pair  $(i, k)$  of nodes was available (apart from the inequality  $E[X_i X_k] \geq E[X_i] E[X_k]$  proved in [24]), the common mean-field argument, assuming independence and leading to the approximation  $E[X_i X_k] \approx E[X_i] E[X_k]$ , was a best possible guess. Our estimate  $\Sigma_\infty$  of the correlation structure thus adds crucial new information to the theory of SIS epidemics on networks.

## 2 Non-negative matrix factorization

In recent years, a lot of attention has been devoted to NMF. Several good algorithms have been developed to find the matrices  $W$  and  $H$  in  $\mathbb{R}_+^{k \times n}$  that minimise given objective functions such as the Frobenius norm  $\|\tilde{A} - W^T H\|$  (see e.g. [18, p. 234]). A particularity of our specific problem is that the diagonal of  $\tilde{A}$  is zero and irrelevant (there is no self-infection), which may lead to different objective functions and possibly adapted algorithms for finding  $W$  and  $H$ . In the case where  $\tilde{A}$  is symmetric, it is common practice [25] to choose  $H = W$ , but we will not impose this equality in general. In the sequel, we will assume that NMF algorithms will supply us with the matrices  $W$  and  $H$  such that  $W^T H$  approximates  $\tilde{A}$ , except possibly on the diagonal.

After this first approximation, we continue by assuming that  $\tilde{A} = W^T H$  outside of the diagonal. Denote the  $k \times n$  matrices  $W = \begin{bmatrix} W_1 & W_2 & \cdots & W_n \end{bmatrix}$  and  $H = \begin{bmatrix} H_1 & H_2 & \cdots & H_n \end{bmatrix}$ , where  $W_i$  and  $H_i$  are real  $k \times 1$  vectors. The infection rate at which node  $i$  infects node  $j$  is then given by the inner product of the vectors  $W_i$  and  $H_j$ :

$$\tilde{a}_{ij} = \beta_{ij} a_{ij} = W_i^T H_j \quad (2)$$

We therefore call  $W_i$  the “infectiousness” of node  $i$ , and  $H_j$  the “susceptibility” of node  $j$ . The

final characteristic of a node  $i$  is its healing rate  $\delta_i$ . Hence, each node  $i$  is characterized by a vector  $Z_i \in \mathbb{R}_+^{2k+1}$ , with

$$Z_i = \begin{pmatrix} \sqrt{n} W_i \\ \sqrt{n} H_i \\ \delta_i \end{pmatrix}. \quad (3)$$

The scaling by  $\sqrt{n}$  of the two vectors  $W_i$  and  $H_i$  is useful later on in Section 4. If two nodes  $i$  and  $j$  have the same “Z-vector” (so  $Z_i = Z_j$ ), then these two nodes become indistinguishable in the SIS process. Analogous to the complete graph, this means that the reduced process where we only remember how many of those nodes with equal “Z-vector” are infected, is still a Markov process. If  $n \gg k$ , then there are many Z-vectors in  $\mathbb{R}_+^{2k+1}$ , implying that many of the  $n$  nodes are almost indistinguishable and such indistinguishable nodes can be clustered and represented by a single Z-vector.

Let us choose  $r$  clusters  $C_j \subset \{1, \dots, n\}$  of nodes such that (a) their union  $\cup_{j=1}^r C_j = \{1, \dots, n\}$  comprises all the nodes in the graph  $G$  and (b) clusters are not overlapping, i.e.  $C_j \cap C_l = \emptyset$  if  $j \neq l$ , meaning that two different clusters do not share a node. We define by  $n_j$  the number of nodes in cluster  $C_j$  and we call  $Y_j$  the *cluster center*, defined as

$$Y_j = \frac{1}{n_j} \sum_{i \in C_j} Z_i \quad (4)$$

which equals the average of all Z-vectors in cluster  $j$ . Ideally, we want to choose the  $r$  clusters in such a way that almost all nodes have their Z-vector reasonably close to their corresponding cluster center  $Y_j$ . Intuitively, the number  $r$  of clusters must be sufficiently large such that each cluster center  $Y_j$  is a reasonable approximation for most nodes in the cluster  $C_j$ . However,  $r$  should not be too large, otherwise the number of nodes in each cluster may not be large enough. It will turn out that this last requirement is not as essential as being close to the cluster center.

Once the set of clusters  $\{C_j\}_{1 \leq j \leq r}$  is determined, we propose a new “clustered SIS” model, that approximates the original Markovian *heterogeneous* SIS process, by replacing the  $Z_i$ -vector of each node  $i \in C_j$  by its corresponding cluster center  $Y_j$ . In other words, we replace  $Z_i$  by

$$\tilde{Z}_i = \sum_{j=1}^r 1_{\{i \in C_j\}} Y_j,$$

and any node  $i$  belonging to the same cluster  $C_j$  thus possesses the same  $\tilde{Z}_i = Y_j$ . In our new approximate “clustered SIS” model, all nodes belonging to the same cluster are indistinguishable. Hence, the random vector  $N = (N_1, \dots, N_r)$  containing the number  $N_j$  of infected nodes (with  $0 \leq N_j \leq n_j$ ) in each cluster  $C_j$  is a continuous-time Markov process! We will study this Markov process in more detail.

### 3 The Markov process $N = (N_1, \dots, N_r)$

We introduce the following notation: we split up any vector  $y \in \mathbb{R}^{2k+1}$  according to the block vector structure of  $Z_i$ ,

$$y = \begin{pmatrix} y_w \\ y_h \\ y_\delta \end{pmatrix},$$

where the vector  $y_w \in \mathbb{R}^k$  corresponds to  $\sqrt{n}$  times the infectiousness, the vector  $y_h \in \mathbb{R}^k$  corresponds to  $\sqrt{n}$  times the susceptibility and the scalar  $y_\delta$  corresponds to the healing rate. In particular, the

cluster center is denoted by  $Y_j = \begin{pmatrix} Y_{w,j} \\ Y_{h,j} \\ Y_{\delta,j} \end{pmatrix}$ .

The generator of the process  $N(t)$  is determined by the possible transition rates:

$$N_j \longrightarrow N_j + 1 \text{ at rate } \frac{1}{n} \sum_{l=1}^r (n_j - N_j) N_l Y_{w,l}^T Y_{h,j} \quad (5)$$

while

$$N_j \longrightarrow N_j - 1 \text{ at rate } N_j Y_{\delta,j}. \quad (6)$$

In our new approximate ‘‘clustered SIS’’ model, the number  $N_j$  of infected nodes in cluster  $C_j$  increases as in (5), because each of the  $N_l$  infected nodes in cluster  $C_l$  can infect a healthy node of the total  $n_j - N_j$  healthy nodes in cluster  $C_j$  at rate equal to  $\frac{1}{n} Y_{w,l}^T Y_{h,j}$ , which even holds true for  $l = j$ . The rate equation (6) means that each of the  $N_j$  infected nodes in cluster  $C_j$  can heal with rate  $Y_{\delta,j}$ . The number  $N_j$  of infected nodes in cluster  $C_j$  follows a birth-death process [11], in which the birth rates depend upon the number  $N_l$  of infected nodes in any cluster  $C_l$ , including  $C_j$  itself. In fact, the new approximate ‘‘clustered SIS’’ model for the vector  $N$ , that approximates the number of infected nodes in  $G$ , consists of  $r$  birth-death processes, coupled to each other through the infection rates  $\frac{1}{n} Y_{w,l}^T Y_{h,j}$  from cluster  $C_l$  to  $C_j$ .

Clearly, the state space of the continuous-time process  $N(t) = (N_1(t), \dots, N_r(t))$ , in which the integer random variable  $N_j(t)$  changes with time  $t$ , equals the product  $\bigotimes_{j=1}^r \{0, 1, 2, \dots, n_j\}$  of possible infection states per cluster  $C_j$ . We now embed this state space in  $\mathbb{R}_+^r$  to allow the computation with real, rather than integer  $r \times 1$  vectors. In particular, the metastable state of the new approximate ‘‘clustered SIS’’ model is obtained for a real vector  $N^\infty \in \mathbb{R}_+^r$  when, for each component  $N_j$ , the rate of increase by one equals the rate of decrease by one. These equalities are commonly called the balance equations for the steady state in a continuous-time Markov process [11, p. 213-214]. The vector  $N^\infty$  represents the expected number of infected nodes per cluster in meta-stable equilibrium. Equating the rate equations (5) and (6) yields

$$\forall j \in \{1, \dots, r\} : \frac{1}{n} \sum_{l=1}^r (n_j - N_j^\infty) N_l^\infty Y_{w,l}^T Y_{h,j} = N_j^\infty Y_{\delta,j}. \quad (7)$$

which is an  $r$ -dimensional vector equation, whose solution is shown to exist below. If  $k < r$ , we can solve these equations in the following way: define the vector  $V \in \mathbb{R}^k$  by

$$V = \frac{1}{n} \sum_{l=1}^r N_l^\infty Y_{w,l}. \quad (8)$$

Then (7) becomes

$$\forall j \in \{1, \dots, r\} : (n_j - N_j^\infty) V^T Y_{h,j} = N_j^\infty Y_{\delta,j}.$$

from which it follows that

$$N_j^\infty = n_j \cdot \frac{V^T Y_{h,j}}{V^T Y_{h,j} + Y_{\delta,j}}. \quad (9)$$

It remains to determine the vector  $V$ . Substituting (9) into the definition (8) of  $V$  yields the recursion

$$V = \frac{1}{n} \sum_{l=1}^r n_l \cdot \frac{Y_{w,l} Y_{h,l}^T V}{Y_{h,l}^T V + Y_{\delta,l}}. \quad (10)$$

So we have reduced the  $r$ -dimensional equation (7) to a  $k$ -dimensional equation. This  $k$ -dimensional vector equation (10) in  $V$  can numerically be solved efficiently, even for relatively large  $k$ , provided a solution exists.

### 3.1 Existence of the metastable state

We will now write the equation (7) for the metastable state in matrix form. Let us first define  $\mathbf{n}$  as the vector  $(n_1, \dots, n_r)$  with the number of nodes in each cluster and denote the  $k \times r$  matrices

$$Y_w = \begin{bmatrix} Y_{w,1} & \cdots & Y_{w,r} \end{bmatrix} \text{ and } Y_h = \begin{bmatrix} Y_{h,1} & \cdots & Y_{h,r} \end{bmatrix}.$$

In addition, we use the following notation for a vector  $a \in \mathbb{R}^p$ :

$$\text{diag}(a) = \begin{pmatrix} a_1 & & \\ & \ddots & \\ & & a_p \end{pmatrix}.$$

Then, (7) becomes

$$\frac{1}{n} \text{diag}(\mathbf{n}) Y_h^T Y_w N^\infty - \frac{1}{n} \text{diag}(N^\infty) Y_h^T Y_w N^\infty = \text{diag}(Y_\delta) N^\infty$$

and

$$\begin{aligned} 0 &= \left\{ \frac{1}{n} \text{diag}(\mathbf{n}) Y_h^T Y_w - \text{diag}(Y_\delta) \right\} N^\infty - \frac{1}{n} \text{diag}(N^\infty) Y_h^T Y_w N^\infty \\ &= \text{diag}(Y_\delta) \left\{ \frac{1}{n} \text{diag}(\mathbf{n}/Y_\delta) Y_h^T Y_w - I \right\} N^\infty - \frac{1}{n} \text{diag}(N^\infty) Y_h^T Y_w N^\infty \end{aligned}$$

After denoting the non-negative  $r \times r$  matrix

$$\bar{A} = \frac{1}{n} \text{diag}(\mathbf{n}/Y_\delta) Y_h^T Y_w,$$

the balance equation (7) finally becomes

$$0 = \text{diag}(Y_\delta) (\bar{A} - I) N^\infty - \frac{1}{n} \text{diag}(N^\infty) Y_h^T Y_w N^\infty \quad (11)$$

As in [26], we can prove that the metastable state matrix equation (11) has a strictly positive solution in  $N^\infty$  if the  $r \times r$ -matrix  $\bar{A}$  has a positive eigenvalue greater than 1. Indeed, let us assume that all healing rates  $\delta_i = \delta$  are the same, then

$$\bar{A} = \frac{1}{\delta} \frac{1}{n} \text{diag}(\mathbf{n}) Y_h^T Y_w.$$

Furthermore, suppose that each  $Z_i$  is very close to its cluster center, for example, if  $r$  is close to  $n$ . Next, define the map  $\text{Cl} : \{1, \dots, n\} \rightarrow \{1, \dots, r\}$ , such that  $\text{Cl}(i) = j$  precisely when  $i \in C_j$ . Since the  $n \times n$  infection rate adjacency matrix  $\tilde{A}^T = H^T W$ , we can write its elements using the map  $\text{Cl}$  as

$$\tilde{a}_{ii'}^T = H_i^T W_{i'} = \frac{1}{n} (Y_h^T Y_w)_{\text{Cl}(i)\text{Cl}(i')}.$$

Hence, if  $\bar{v} \in \mathbb{R}^r$  is the positive eigenvector of the non-negative matrix  $\bar{A}$  corresponding to the eigenvalue  $\lambda > 1$ , then, after defining  $v \in \mathbb{R}^n$  by

$$v_i = \bar{v}_{\text{Cl}(i)},$$

we arrive at

$$\frac{1}{\delta} (\tilde{A}^T v)_i = \frac{1}{\delta} \sum_{i'=1}^n \tilde{a}_{ii'}^T v_{i'} = \frac{1}{\delta} \sum_{j=1}^r \frac{n_j}{n} (Y_h^T Y_w)_{\text{Cl}(i)j} \bar{v}_j = (\bar{A} \bar{v})_{\text{Cl}(i)} = \lambda v_i,$$

which demonstrates that  $\lambda$  is also an eigenvalue of  $\tilde{A}^T/\delta$ . This means that a metastable solution for  $N^\infty$  exists if the largest eigenvalue  $\lambda$  of  $\tilde{A}^T/\delta$  is larger than 1, which is exactly the same condition that NIMFA [26] predicts in this case!

## 4 Continuous approximation of the process $N$

In this section, we show how our ‘‘clustered SIS’’ Markov process  $N$ , with the transition rates given in (5) and (6), can in turn be approximated by a Markov process with a continuous state space in a classical way, namely by approximating a difference of Poisson processes by a Brownian motion with drift [27].

We center and rescale the process  $N$  and we define the deviations process  $D$  by

$$D = \frac{N - N^\infty}{\sqrt{n}} \tag{12}$$

where the  $\sqrt{n}$ -scaling will become clear later. The transition rates for  $D$  directly follow from (5) and (6),

$$D_j \longrightarrow D_j + 1/\sqrt{n} \text{ at rate } \frac{1}{n} \sum_{l=1}^r (n_j - N_j^\infty - n^{1/2} D_j) (n^{1/2} D_l + N_l^\infty) Y_{w,l}^T Y_{h,j} \tag{13}$$

$$D_j \longrightarrow D_j - 1/\sqrt{n} \text{ at rate } (N_j^\infty + n^{1/2} D_j) Y_{\delta,j}. \tag{14}$$

We now suppose that the number of nodes  $n$  in the graph  $G$  is large. At some time  $t$ , there will be many infection and healing events in a relatively small time interval  $[t, t+h]$ . If  $h$  is so small that the transition rates can be assumed to be constant during the time interval  $[t, t+h]$  (this means that the changes in  $D$  during that time interval are negligible), then the distribution of the number  $I_j(h)$  of nodes in cluster  $C_j$  that become infected during the time interval  $[t, t+h]$  and the number  $H_j(h)$  of nodes in cluster  $C_j$  that heal in that time interval can be determined. To a good approximation, the random variables  $I_j(h)$  and  $H_j(h)$  for each cluster  $1 \leq j \leq r$  will all be independent and Poisson distributed. We can explicitly calculate the expectation of these random variables, conditioned on  $D(t)$ :

$$\mathbb{E}[I_j(h) \mid D(t)] = \frac{h}{n} \sum_{l=1}^r (n_j - N_j^\infty - n^{1/2} D_j) (n^{1/2} D_l + N_l^\infty) Y_{w,l}^T Y_{h,j}$$

and

$$\mathbb{E}[H_j(h) \mid D(t)] = h(N_j^\infty + n^{1/2}D_j)Y_{\delta,j}.$$

Next, we calculate the expectation of the vector  $dD(h) = D(t+h) - D(t) = n^{-1/2}(I(h) - H(h))$ . The  $j$ -th component is

$$\begin{aligned} \mathbb{E}[dD_j(h) \mid D(t)] &= n^{-\frac{1}{2}}(\mathbb{E}[I_j(h) \mid D(t)] - \mathbb{E}[H_j(h) \mid D(t)]) \\ &= hn^{-\frac{1}{2}} \left( \frac{1}{n} \sum_{l=1}^r (n_j - N_j^\infty - n^{1/2}D_j)(n^{1/2}D_l + N_l^\infty)Y_{w,l}^T Y_{h,j} - (N_j^\infty + n^{1/2}D_j)Y_{\delta,j} \right). \end{aligned}$$

Using the metastable state equation (7) yields cancellation of the main order terms:

$$\mathbb{E}[dD_j(h) \mid D(t)] = h \left( \frac{1}{n} \sum_{l=1}^r \left( (n_j - N_j^\infty - n^{1/2}D_j)D_l - D_j N_l^\infty \right) Y_{w,l}^T Y_{h,j} - D_j Y_{\delta,j} \right).$$

Conditionally on  $D(t)$ , the components of  $dD(h)$  are independent, so that we only need to determine the variances. Since the variance of a Poisson distribution is equal to the mean, we add the expectations of  $I_j(h)$  and  $H_j(h)$ ,

$$\begin{aligned} \text{Var}[dD_j(h) \mid D(t)] &= \text{Var} \left[ n^{-\frac{1}{2}}(I_j(h) - H_j(h)) \mid D(t) \right] = \frac{1}{n}(\mathbb{E}[I_j(h) \mid D(t)] - \mathbb{E}[H_j(h) \mid D(t)]) \\ &= \frac{h}{n} \left( \frac{1}{n} \sum_{l=1}^r (n_j - N_j^\infty - n^{1/2}D_j)(n^{1/2}D_l + N_l^\infty)Y_{w,l}^T Y_{h,j} + (N_j^\infty + n^{1/2}D_j)Y_{\delta,j} \right). \end{aligned}$$

and again introducing the metastable state equation (7), we find

$$\text{Var}[dD_j(h) \mid D(t)] = hn^{-\frac{1}{2}} \left( \frac{1}{n} \sum_{l=1}^r \left( (n_j - N_j^\infty - n^{1/2}D_j)D_l - D_j N_l^\infty \right) Y_{w,l}^T Y_{h,j} + (2n^{-\frac{1}{2}}N_j^\infty + D_j)Y_{\delta,j} \right).$$

The addition of the expectations of  $I_j(h)$  and  $H_j(h)$  explains why there is no cancellation of the main order terms of the variance, leading to the term  $2hN_j^\infty Y_{\delta,j}/n$ . Compared to the expectation, there is also an extra factor  $n^{-\frac{1}{2}}$  in the variance. It is convenient to write these equations for each  $1 \leq j \leq r$  in matrix notation as in Section 3.1,

$$\mathbb{E}[dD(h) \mid D(t)] = h \left( \frac{1}{n} \text{diag}(\mathbf{n} - N^\infty - n^{1/2}D)Y_h^T Y_w D - \frac{1}{n} \text{diag}(Y_h^T Y_w N^\infty)D - \text{diag}(Y_\delta)D \right).$$

We introduce the  $r \times r$ -matrix  $M$ ,

$$M = \frac{1}{n} \text{diag}(\mathbf{n} - N^\infty)Y_h^T Y_w - \frac{1}{n} \text{diag}(Y_h^T Y_w N^\infty). \quad (15)$$

and obtain

$$\mathbb{E}[dD(h) \mid D(t)] = h \left( (M - \text{diag}(Y_\delta))D - \frac{1}{\sqrt{n}} \text{diag}(D)Y_h^T Y_w D \right). \quad (16)$$

For the conditional variance of  $dD(h)$ , we find a similar formula:

$$\text{Var}[dD(h) \mid D(t)] = h \left( \frac{1}{\sqrt{n}}(M + \text{diag}(Y_\delta))D - \frac{1}{n} \text{diag}(D)Y_h^T Y_w D + \frac{2}{n} \text{diag}(Y_\delta)N^\infty \right). \quad (17)$$

For large  $n$ , it is natural to consider  $D$  as a continuous process. We have shown that  $dD(h)$  is distributed as the scaled difference of independent Poisson random variables, so that  $dD(h)$  can be

approximated by a normal distribution. Equations (16) and (17) then suggest to model  $D$  as the solution of the following stochastic vector differential equation (SVDE):

$$dD(t) = \left( (M - \text{diag}(Y_\delta)) - \frac{1}{\sqrt{n}} \text{diag}(D(t)) Y_h^T Y_w \right) D(t) dt + \text{diag} \left( \sqrt{\frac{1}{\sqrt{n}} (M + \text{diag}(Y_\delta)) D - \frac{1}{n} \text{diag}(D) Y_h^T Y_w D + \frac{2}{n} \text{diag}(Y_\delta) N^\infty} \right) dB(t). \quad (18)$$

where  $B(t)$  is an  $r$ -dimensional standard Brownian motion, and where we have used the notation for vectors  $a \in \mathbb{R}_+^p$ ,

$$\sqrt{a} = (\sqrt{a_1}, \sqrt{a_2}, \dots, \sqrt{a_p})$$

Equation (18) can be used to efficiently simulate the time-evolution of  $D$ . From such simulation, not only information about the metastable distribution can be obtained, but also about the relaxation time, for example. Since the SVDE in (18) is non-linear in  $D$ , an exact analysis is hard. However, for large  $n$ , we can make additional approximations as shown in Appendix A, that lead us to conclude, provided the largest eigenvalue  $\lambda$  of  $A^T/\delta$  is larger than 1, that the metastable distribution of the vector of infected nodes

$$N = N^\infty + \sqrt{n}D$$

equals an  $r$ -dimensional normal distribution, with expectation equal to  $N^\infty$  (since  $\mathbb{E}[D] = 0$ ), and covariance matrix  $n\Sigma_\infty$  specified in (24).

## 5 Evaluation of the “clustered SIS” model

### 5.1 Choosing the number of clusters $r$

When applying our method to a particular example, we face two problems: we have to choose both the dimension  $k$  of our non-negative matrix factorization of  $\tilde{A}$  and the number  $r$  of clusters. The first problem is hard, and it depends on how well  $\tilde{A}$  can be approximated by the product of two low rank  $k \times n$  matrices  $W$  and  $H$ . Choosing the number  $r$  of clusters is less delicate: if we choose a lot of clusters, but a subset of the cluster centers are very close together, then the clusters themselves become indistinguishable. This means that the total number of infected nodes in the union of the respective subset of clusters behaves as though it were one cluster, also in the approximation of the SVDE. The argument guarantees a certain stability: choosing more clusters does not really change the predicted behavior of a fixed subset of nodes. We therefore recommend choosing a lot of clusters (maybe even  $r = n$ ), since the bias effect is less severe, whereas the effect on the variance is limited, especially for larger collections of nodes. Clearly, on a micro-level (when looking at a few nodes), the approximation will not get much better.

### 5.2 Application to a simulated network

A random network with a power law degree distribution  $\Pr(D_i > x) \sim x^{-2}$ , where  $D_i$  is the degree of node  $i$  in the network, is generated by the configuration model. Only the largest connected component of the generated network is used, consisting of  $n = 9994$  nodes and with a maximum degree of 1229

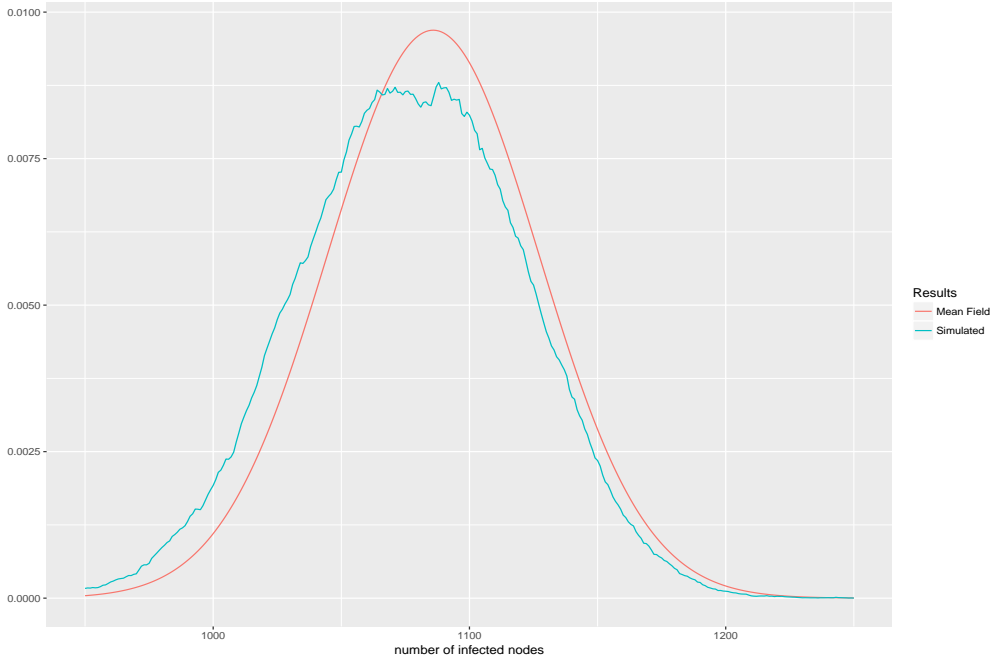


Figure 1: Distribution of number of infected nodes in the simulated network in the metastable state.

and an average degree of 15. The infection rate matrix  $\tilde{A}$  is symmetric, with infection rate  $\beta_{ij} = 1$  between all pairs  $(i, j)$  of connected nodes. We have made a one-dimensional ( $k = 1$ ) factorisation of  $\tilde{A}$ , invoking a fast iterative algorithm that minimises  $\sum_{i=1}^n \sum_{j=1}^n \omega_{ij} (\tilde{a}_{ij} - W_i^T H_j)^2$ . We take weights  $\omega_{ij}$  of the form  $\omega_{ii} = 0$  (the diagonal of  $\tilde{A}$  is irrelevant) and  $\omega_{ij} = e^{\lambda \tilde{a}_{ij}}$  ( $i \neq j$ ), where we can still tune the parameter  $\lambda \in \mathbb{R}$ . In the current example,  $\tilde{A}$  is a 0-1-matrix, so for  $i \neq j$  there are only two possible weights:  $w_{ij} = 1$  if  $\tilde{a}_{ij} = 0$  and  $w_{ij} = e^\lambda$  if  $\tilde{a}_{ij} = 1$ . The parameter  $\lambda$  allows us to control the “best” approximation  $W^T H$  for  $\tilde{A}$ , since we have no theoretical results guiding us in this approximation. Here we choose  $\lambda$  in such a way that the NIMFA approximation of the expected total number of infected nodes for the network with matrix  $W^T H$  is (approximately) equal to the original NIMFA approximation.

In the one dimensional approximation of the symmetric matrix  $\tilde{A}$ , it comes out of the minimization procedure that also  $W^T H$  will be symmetric, i.e. we can choose the  $n \times 1$  matrix  $W$  equal to  $H$  and we base our clustering solely on  $W$ . We choose  $r = 100$  clusters, where we put a few large values of  $W$  in separate clusters. The metastable state number of infected nodes in our “clustered SIS” model is computed from (9) and (10), and the covariance matrix for all 100 clusters is approximated by  $n\Sigma_\infty$ , specified in (24). Figure 1 shows how well our 1-dimensional approximation is able to estimate the distribution of the total number of infected nodes, which we obtained via simulation of the entire network with infection matrix  $\tilde{A}$ . The simulations started with all nodes infected. Only when the metastable regime is approximately reached, the simulation data is collected for a long time to accurately obtain the metastable distribution of the infected nodes. The accuracy of the  $k = 1$  approximation is also illustrated by the following table. From the simulated distribution in the metastable state, the expectation and standard deviation of the number of infected nodes in the graph

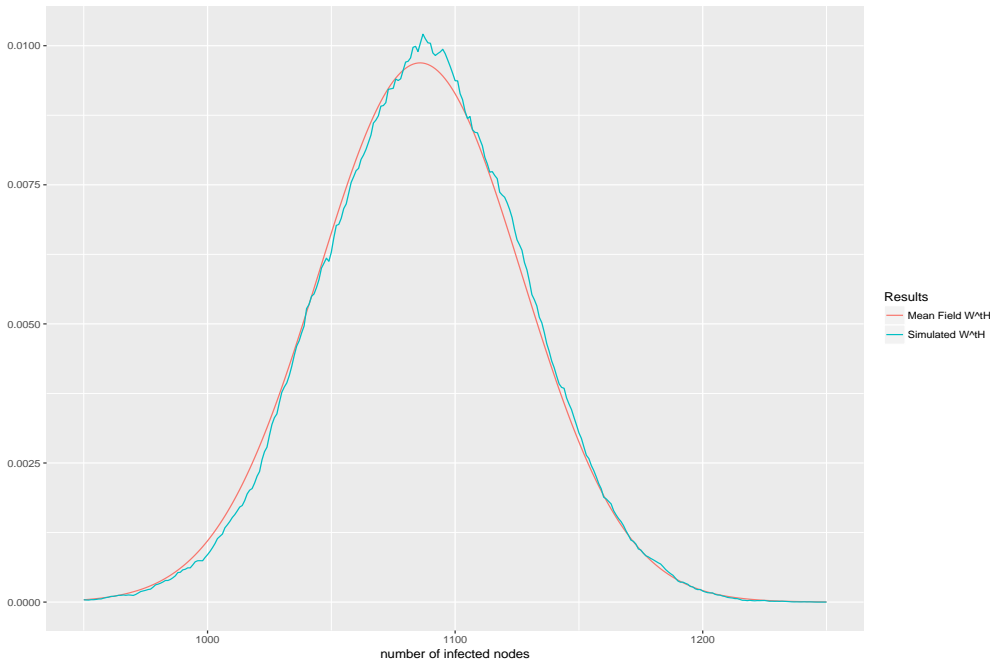


Figure 2: Distribution of number of infected nodes in the  $W^T H$ -network

are computed in the first column and compared with the mean  $u^T N^\infty$  in (9), where  $u$  is the all-one vector, and the standard deviation  $\sqrt{n} \cdot \sqrt{u^T \Sigma_\infty u}$  in (24) in the last column. Note that this standard deviation depends on the clustering and is also used for plotting the curve in Figure 1, as the mean field approximation only gives the center of the distribution.

	Simulated	Mean Field
Expectation	1076.0	1085.9
Standard Deviation	43.7	41.16

NIMFA [11, Chapter 17] provides an upper bound of viral infection probability of a node. This causes the expectation to be overestimated by NIMFA. This overestimation is by construction still present in the curve in Figure 1, but the estimation of the variance is rather good.

Our approach makes several approximations: (a) the infection rate matrix  $\tilde{A}$  is approximated by  $W^T H$ , which we further call the  $W^T H$ -network, (b) clusters are chosen and (c) finally, the dynamics in each cluster is described by a continuous Markov process  $N$  as explained in Section 3. To assess the effects of these approximations, we have also simulated directly from the  $W^T H$ -network in the same way as before, but now using  $W^T H$  as infection rate matrix, to compare this with our predicted results. The results are astonishingly accurate, as demonstrated in Figure 2. The predicted curve is the same as in Figure 1 and is very close to the  $W^T H$ -simulation. This means that for the  $W^T H$ -network the clustering and continuous approximation work really well; in Figure 2 there is even no visible NIMFA bias. Notably, even the one-dimensional approach ( $k = 1$ ) is capable to approximate the variance well.

The main issue that remains is the bias in the prediction for the original network. In the next

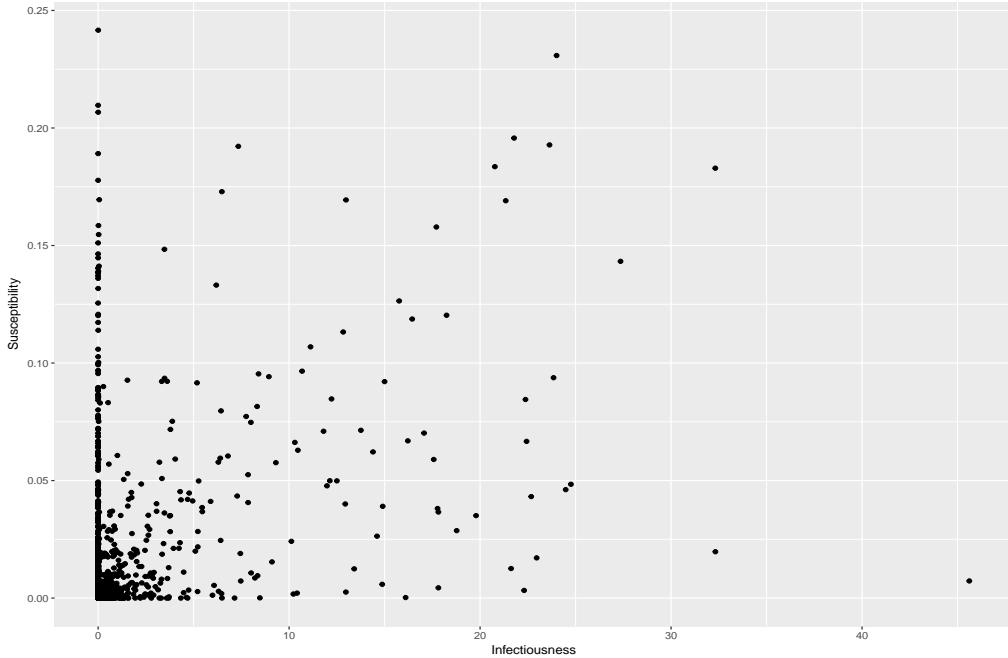


Figure 3: Scatter plot of  $W$  and  $H$  in the air weight network

paragraph, we will present a method to correct for this NIMFA bias, that, unfortunately, requires a high number of clusters and a high-dimensional approximation, which was unfeasible to compute for this large network.

### 5.3 Application to a real-world network

We consider the airline network (with  $n = 3425$  nodes and  $L = 15358$  links), where the nodes are the airports and the infection rate  $\beta_{ij}$  along a link is proportional to the number of flights between the two airports. Qu and Wang [28] have constructed this network and its infection rates from the dataset of openflights<sup>1</sup>. Many of the asymmetric infection rates ( $\beta_{ij} \neq \beta_{ji}$ ) are zero; thus many nodes<sup>2</sup> have zero infectiousness (zero out-degree) or zero susceptibility (zero in-degree). This means that the susceptibility and the infectiousness of a node are actually different.

As before, we start by making a one dimensional factorization, resulting in a vector  $W$  and  $H$ , where we force the NIMFA approximations for the original and factorized matrix to be approximately equal. Figure 3 gives an impression of  $W$  and  $H$ . Clustering is not so obvious. Since the network is relatively small, we decided to choose  $n$  clusters: each node becomes a separate cluster. However, the expected prevalence for each node (the vector  $N^\infty$ ) and the estimated covariance matrix  $\Sigma_\infty$  are not

<sup>1</sup><https://openflights.org/data.html>

<sup>2</sup>In fact, there are precisely 348 nodes with zero in- and out-degree. Those nodes have been omitted by Qu and Wang [28]. Our approach can handle such zero in- and zero out-degree nodes.

very impressive:

	Simulated	Mean Field
Expectation	1105.8	1135.1
Standard Deviation	29.4	16.45

There is a sizeable overestimation of the expectation and a severe underestimation of the variance. These differences are caused by the fact that in this case  $\tilde{A}$  is rather poorly approximated by the rank-one matrix  $W^T H$ . Apparently in some cases a one-dimensional factorization works pretty well, but for the current example clearly not. Additional research is needed to be able to predict performance of low-dimensional factorizations from network properties.

To improve our results for this network, we need to increase the dimension  $k$ . In fact, since the network is small, we do not need to approximate  $\tilde{A}$  with a lower rank factorization at all: we simply use  $\tilde{A}$  itself in our formula's (for example, choose  $H = \tilde{A}$  and  $W = I$  the identity matrix, and therefore  $k = n$ ). Furthermore, each node in the network consists of its own cluster. We also perform a correction on the NIMFA expectations  $N^\infty$  in the following way. NIMFA upper bounds the infection probability per node: in governing equation (1), NIMFA replaces  $E[X_i X_k]$  by  $E[X_i] E[X_k]$ , ignoring the positive covariance between  $X_i$  and  $X_k$ . However, the matrix  $\Sigma_\infty$  provides an indication of the covariance between any two nodes! We now use the following procedure: after determining  $N^\infty$  using equations (9), we determine  $\Sigma_\infty$  using (24). Then, we determine a *corrected vector*  $\hat{N}^\infty$  of cluster expectations by adjusting the cluster rate equations (5) and (6):

$$\begin{aligned}
\frac{dE[N_j]}{dt} &= \frac{1}{n} \sum_{l=1}^r E[(n_j - N_j) N_l] Y_{w,l}^T Y_{h,j} - E[N_j] Y_{\delta,j} \\
&= \frac{1}{n} \sum_{l=1}^r (n_j - E[N_j]) E[N_l] Y_{w,l}^T Y_{h,j} - E[N_j] Y_{\delta,j} - \frac{1}{n} \sum_{l=1}^r \text{Cov}(N_j, N_l) Y_{w,l}^T Y_{h,j} \\
&\approx \frac{1}{n} \sum_{l=1}^r (n_j - E[N_j]) E[N_l] Y_{w,l}^T Y_{h,j} - E[N_j] Y_{\delta,j} - \frac{1}{n} \sum_{l=1}^r \Sigma_{\infty, jl} Y_{w,l}^T Y_{h,j}. \tag{19}
\end{aligned}$$

We find the metastable expectation by equating the time derivative to zero ( $\frac{dE[N_j]}{dt} = 0$ ). Hence, the corrected metastable state expectation  $E[N_j^\infty] = \hat{N}_j^\infty$  in cluster  $j$  is determined by

$$\forall 1 \leq j \leq r : \frac{1}{n} \sum_{l=1}^r (n_j - \hat{N}_j^\infty) \hat{N}_l^\infty Y_{w,l}^T Y_{h,j} - \hat{N}_j^\infty Y_{\delta,j} - \frac{1}{n} \sum_{l=1}^r \Sigma_{\infty, jl} Y_{w,l}^T Y_{h,j} = 0.$$

The expectation of a few nodes might turn out to be slightly negative with this method, so we replace those by zero to obtain the corrected mean-field approximation. It turns out that this correction is negligible (compared to the original  $N^\infty$ ) when using a low-dimensional  $k$  factorisation approximation of  $\tilde{A}$ . However, in this example (using  $r = n$  and  $k = n$ ), we found the following result:

	Simulated	Mean-field	Corrected Mean-field
Expectation	1105.8	1136.1	1104.0
Standard Deviation	29.4	27.7	27.7

By construction, the mean field expectation is still about the same, but the corrected version is much more accurate. We also tried to iteratively update  $\Sigma_\infty$  using the corrected expectation, but this did

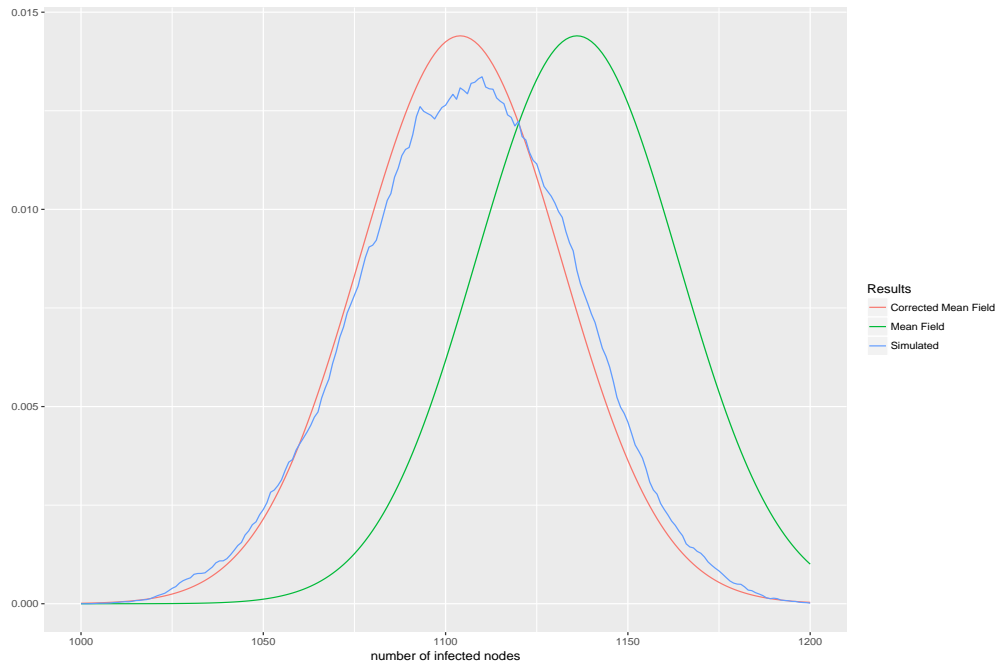


Figure 4: Distribution of number of infected nodes in Air Weight network

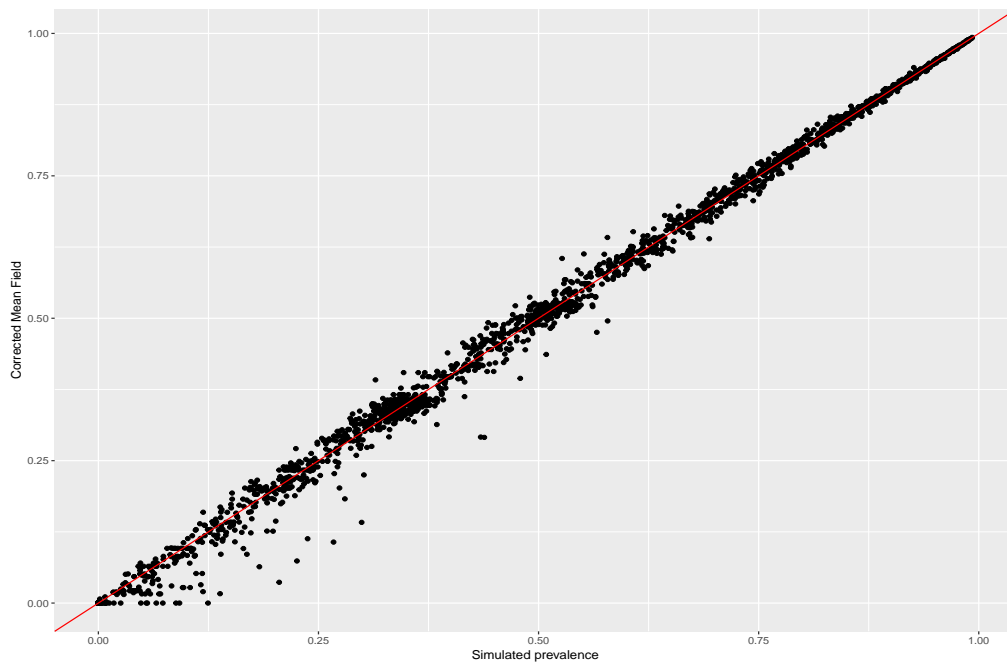


Figure 5: Infection probability of each node in Air Weight network

not give substantial improvements. Figure 4 shows the good fit of the normal distribution, while Figure 5 assesses the quality of the corrected mean-field approximation against simulations. We are not only able to substantially improve NIMFA, but we are also able to obtain a rather precise indication of variances and covariances. We ought to mention that our correction method is infeasible for very large networks; there we would need to approximate  $\tilde{A}$  by a low rank non-negative matrix factorisation. We advise to take  $k$  as high as possible, and to take the number of clusters  $r$  as high as possible.

## 6 Discussion

Our analysis resembles a reaction-diffusion process studied in meta-populations as outlined in [1, Section IX]. Instead of immediately assuming a mean-field approach as in reaction-diffusion models [1, Section IX], our “clustered SIS” model makes the following approximations. First, we assume that the infection rate matrix can be factorized as  $\tilde{A}_{n \times n} = (W^T)_{n \times k} H_{k \times n}$  with a tuneable  $k$  (which can incur an approximation [16] if  $k$  is small compared to  $n$ ). Second, we assume that  $r$  clusters can be found for which the cluster center represents the infectious state ( $Z$ -vector) for all nodes in the same cluster well. After these two assumptions (that may lead to approximations), a discrete Markov process  $N$  arises, whose metastable state can be obtained. Moreover, that metastable state  $N^\infty$  exists provided that the largest eigenvalue  $\lambda$  of  $\tilde{A}^T/\delta$  exceeds 1, precisely agreeing with earlier mean-field approximations (NIMFA) in heterogeneous epidemics. Third, by additionally approximating the discrete Markov chain  $N$  by a continuous Brownian motion, a stochastic, non-linear vector differential equation (18) is deduced, whose linearization (which is a fourth approximation and presented in Appendix A) for large population sizes can be solved exactly, from which a Gaussian vector distribution (with mean and covariances) of the number of infected nodes per cluster is obtained.

In spite of several approximations in the “clustered SIS” model, its accuracy, assessed in Section 5, is remarkably good in synthetic graphs even for low dimensional factorizations. These low dimensional factorizations are less sharp in a real-world airport network, but bypassing the factorization and many clusters, we were also able to predict the meta-stable distribution very well. Motivated to increase the overall performance of the “clustered SIS” model, we found an efficient method to adjust the NIMFA bias by utilizing the asymptotic covariance matrix  $\Sigma_\infty$ , defined in (22) and computed in (24). In essence, rather than neglecting pair-correlations as in NIMFA, we approximate in SIS governing equation (1) the pair-correlations by the asymptotic covariance matrix  $\Sigma_\infty$ . This new correction method seems to be surprisingly accurate, which, we hope, will inspire others to test and use it further in the future.

**Acknowledgements.** We are grateful to Huijuan Wang and Bo Qu for the construction of the weighted airport network in Section 5.3 from the dataset of openflights<sup>3</sup>.

## References

- [1] R. Pastor-Satorras, C. Castellano, P. Van Mieghem, and A. Vespignani. Epidemic processes in complex networks. *Review of Modern Physics*, 87(3):925–979, September 2015.

---

<sup>3</sup><https://openflights.org/data.html>

- [2] P. Van Mieghem. Universality of the SIS prevalence in networks. Delft University of Technology, Report20161006 ([www.nas.ewi.tudelft.nl/people/Piet/TUDELFTReports](http://www.nas.ewi.tudelft.nl/people/Piet/TUDELFTReports)); *arXiv:1612.01386*, 2016.
- [3] N. T. J. Bailey. *The Mathematical Theory of Infectious Diseases and its Applications*. Charlin Griffin & Company, London, 2nd edition, 1975.
- [4] R. M. Anderson and R. M. May. *Infectious Diseases of Humans: Dynamics and Control*. Oxford University Press, Oxford, U.K., 1991.
- [5] D. J. Daley and J. Gani. *Epidemic modelling: An Introduction*. Cambridge University Press, Cambridge, U.K., 1999.
- [6] O. Diekmann, H. Heesterbeek, and T. Britton. *Mathematical Tools for Understanding Infectious Disease Dynamics*. Princeton University Press, Princeton, USA, 2012.
- [7] I. Z Kiss, J. C. Miller, and P. L Simon. *Mathematics of network epidemics: from exact to approximate models*. Springer, 2016.
- [8] P. Van Mieghem and R. van de Bovenkamp. Non-Markovian infection spread dramatically alters the SIS epidemic threshold in networks. *Physical Review Letters*, 110(10):108701, March 2013.
- [9] E. Cator, R. van de Bovenkamp, and P. Van Mieghem. Susceptible-Infected-Susceptible epidemics on networks with general infection and curing times. *Physical Review E*, 87(6):062816, June 2013.
- [10] E. Cator and P. Van Mieghem. Second order mean-field SIS epidemic threshold. *Physical Review E*, 85(5):056111, May 2012.
- [11] P. Van Mieghem. *Performance Analysis of Complex Networks and Systems*. Cambridge University Press, Cambridge, U.K., 2014.
- [12] P. Van Mieghem, J. Omic, and R. E. Kooij. Virus spread in networks. *IEEE/ACM Transactions on Networking*, 17(1):1–14, February 2009.
- [13] P. Van Mieghem and E. Cator. Epidemics in networks with nodal self-infections and the epidemic threshold. *Physical Review E*, 86(1):016116, July 2012.
- [14] E. Cator and P. Van Mieghem. Susceptible-Infected-Susceptible epidemics on the complete graph and the star graph: Exact analysis. *Physical Review E*, 87(1):012811, January 2013.
- [15] R. Diestel. *Graph Theory*. Springer-Verlag, Heidelberg, fourth edition, 2010.
- [16] J Hannah and T. J. Laffey. Nonnegative factorization of completely positive matrices. *Linear Algebra and its Applications*, 55:1–9, 1983.
- [17] S. Bonaccorsi, S. Ottaviano, F. De Pellegrini, A. Socievole, and P. Van Mieghem. Epidemic outbreaks in two-scales community networks. *Physical Review E*, 90(1):012810, 2014.
- [18] P. Van Mieghem. *Graph Spectra for Complex Networks*. Cambridge University Press, Cambridge, U.K., 2011.
- [19] S. Bonaccorsi, S. Ottaviano, D. Mugnolo, and F. De Pellegrini. Epidemic outbreaks in networks with equitable or almost-equitable partitions. *SIAM Journal of Applied Mathematics*, 75(6):2421–2443, 2015.
- [20] K. Devriendt and P. Van Mieghem. Universal mean-field framework for SIS epidemics on networks, based on graph partitioning and the isoperimetric inequality. *arXiv: 1706.10132*, 2017.
- [21] P. Van Mieghem. The N - Intertwined SIS epidemic network model. *Computing*, 93(2):147–169, 2011.
- [22] R. Pastor-Satorras and A. Vespignani. Epidemic dynamics and endemic states in complex networks. *Physical Review E*, 63:066117, 2001.
- [23] D. D. Lee and H. S. Seung. Learning the parts of objects by non-negative matrix factorization. *Nature*, 401:788–791, October 1999.
- [24] E. Cator and P. Van Mieghem. Nodal infection in Markovian SIS and SIR epidemics on networks are non-negatively correlated. *Physical Review E*, 89(5):052802, 2014.
- [25] A Vandaele, N. Gillis, Q. Q. Lei, K. Zhong, and I. S. Dhillon. Efficient and non-convex coordinate descent for symmetric nonnegative matrix factorization. *IEEE Transactions on Signal Processing*, 64(21):5571–5581, 2016.

- [26] P. Van Mieghem and J. Omic. In-homogeneous virus spread in networks. Delft University of Technology, Report2008081 ([www.nas.ewi.tudelft.nl/people/Piet/TUdelftReports](http://www.nas.ewi.tudelft.nl/people/Piet/TUdelftReports)); arXiv:1306.2588, 2008.
- [27] J. M. Harrison. *Brownian Motion and Stochastic Flow Systems*. Krieger Publishing Company, Malabar, Florida, 1990.
- [28] B. Qu and H. Wang. SIS epidemic spreading with heterogeneous infection rates. *IEEE Transactions on Network Science and Engineering*, DOI: 10.1109/TNSE.2017.2709786, 2017.
- [29] B. Qu and H. Wang. SIS epidemic spreading with correlated heterogeneous infection rates. *Physica A*, 472:13–24, 2017.

## A Linearising the SVDE (18) for large $n$

Each node is characterised by its infectiousness, susceptibility and healing rate, captured by the vector  $Z_i$  in (3). As the number of nodes  $n$  increases, the average infection rate between two nodes has to decrease, in order for a reasonable metastable state to exist (otherwise all nodes will be infected at almost any time). An asymptotic analysis for large  $n$  requires us to describe how the network grows with  $n$ . Therefore, we suppose that we can model the vectors  $Z_i$  as a sample of size  $n$  from a distribution  $\mu$  on  $\mathbb{R}^{2k+1}$ :

$$\begin{pmatrix} \sqrt{n}W_i \\ \sqrt{n}H_i \\ \delta_i \end{pmatrix} \sim \mu.$$

Since our new approximate ‘‘clustered SIS’’ model only looks at the inner products of  $W_i$  and  $H_j$ , we can always ensure that  $W$  and  $H$  ‘‘live’’ at the same scale. Now, we partition  $\mathbb{R}_+^{2k+1}$  into  $r$  disjoint sets  $\Upsilon_1, \dots, \Upsilon_r$  of positive  $\mu$ -mass, such that their ‘‘centers of mass’’ have small average distance to the other points in the set. If we denote

$$\rho_j = \mu(\Upsilon_j) \text{ and } \tilde{Y}_j = \frac{1}{\rho_j} \int_{\Upsilon_j} y \mu(dy).$$

then our clusters  $C_1, \dots, C_r$  are defined by

$$i \in C_j \iff \begin{pmatrix} \sqrt{n}W_i \\ \sqrt{n}H_i \\ \delta_i \end{pmatrix} \in \Upsilon_j.$$

Approximating  $n_j/n \approx \rho_j$  yields

$$Y_{w,j} = \frac{\sqrt{n}}{n_j} \sum_{i \in C_j} W_i \approx \tilde{Y}_{w,j} \text{ and } Y_{h,j} = \frac{\sqrt{n}}{n_j} \sum_{i \in C_j} H_i \approx \tilde{Y}_{h,j}$$

and

$$Y_{\delta,j} = \frac{1}{n_j} \sum_{i \in C_j} \delta_i \approx \tilde{Y}_{\delta,j}.$$

which shows that the matrix  $Y_h^T Y_w$  tends to  $\tilde{Y}_h^T \tilde{Y}_w$  when  $n \rightarrow \infty$  by the strong law of large numbers [11, p. 119], since  $n = \sum_{j=1}^r n_j$ .

We return to the metastable state equation (7) and define the  $r \times 1$  vector  $\tilde{N}^\infty \in [0, \rho_1] \times \dots \times [0, \rho_r]$  by the equations

$$\forall j \in \{1, \dots, r\} : \sum_{l=1}^r (\rho_j - \tilde{N}_j^\infty) \tilde{N}_l^\infty \tilde{Y}_{w,l}^T \tilde{Y}_{h,j} = \tilde{N}_j^\infty \tilde{Y}_{\delta,j}.$$

Dividing the metastable state equation (7) by  $n$  shows that for large  $n$ ,

$$N^\infty \approx n \tilde{N}^\infty.$$

A closer look at the SVDE (18) reveals that we only need to consider the matrix  $M$  in (15) as  $n \rightarrow \infty$ :

$$\begin{aligned} M &= \frac{1}{n} \text{diag}(\mathbf{n} - N^\infty) Y_h^T Y_w - \frac{1}{n} \text{diag}(Y_h^T Y_w N^\infty) \\ &\approx \text{diag}(\rho - \tilde{N}^\infty) \tilde{Y}_h^T \tilde{Y}_w - \text{diag}(\tilde{Y}_h^T \tilde{Y}_w \tilde{N}^\infty), \end{aligned}$$

illustrating that  $M$  also stabilises or converges. Thus, as  $n \rightarrow \infty$ , the SVDE (18) reduces to

$$dD(t) = (M - \text{diag}(Y_\delta))D(t)dt + \text{diag} \left( \sqrt{2\text{diag}(Y_\delta)N^\infty/n} \right) dB(t). \quad (20)$$

This resulting SVDE (20) is a standard linear SVDE in  $D$ , with a constant diagonal covariance factor!

### A.1 Exact solution of SVDE (20)

Here, we demonstrate that the SVDE (20) can be solved exactly. After defining the  $r \times r$  matrices

$$K = M - \text{diag}(Y_\delta) \text{ and } \Sigma = \text{diag} (2\text{diag}(Y_\delta)N^\infty) /n,$$

from (15) and (9), the SVDE (20) transforms into

$$dD(t) = KD(t)dt + \sqrt{\Sigma} dB(t), \quad (21)$$

and we obtain [27]

$$D(t) = e^{tK}D(0) + \int_0^t e^{(t-s)K} \sqrt{\Sigma} dB(s).$$

Since we are interested in the metastable solution, the eigenvalues of  $K$  must have negative real part, so that

$$\lim_{t \rightarrow \infty} e^{tK}D(0) = 0.$$

Also, the asymptotic covariance will be given by

$$\Sigma_\infty = \lim_{t \rightarrow \infty} \text{Cov} [D(t)] = \int_0^\infty e^{sK} \Sigma (e^{sK})^T ds. \quad (22)$$

There is another way to determine  $\Sigma_\infty$ : when we are in the metastable state (and  $n \rightarrow \infty$ ), the distribution of  $D(t)$  should not depend anymore on  $t$ . Thus, we may suppose that the metastable state is given by

$$D(t) \sim N(\mu, \Sigma_\infty).$$

Invoking (20) shows that  $D(t + dt) = D(t) + dD(t)$  also has a normal distribution. Furthermore,

$$E [dD(t)] = K\mu dt + \sqrt{\Sigma} E [dB(t)] = K\mu dt.$$

So  $\mu = 0$  implies that the expectation is stable. Furthermore, since  $dB(t)$  is independent of the past, we find

$$\begin{aligned} \text{Cov} [D(t + dt)] &= \text{Cov} \left[ D(t) + KD(t)dt + \sqrt{\Sigma} dB(t) \right] \\ &= \text{Cov} [(I + Kdt)D(t)] + \Sigma dt \\ &= (I + Kdt)\Sigma_\infty(I + K^T dt) + \Sigma dt \\ &= \Sigma_\infty + (K\Sigma_\infty + \Sigma_\infty K^T + \Sigma)dt + O(dt^2). \end{aligned}$$

In the metastable state,  $\text{Cov} [D(t + dt)] = \text{Cov} [D(t)]$ . Metastability thus implies that

$$K\Sigma_\infty + \Sigma_\infty K^T + \Sigma = 0. \quad (23)$$

One may verify<sup>4</sup> that  $\Sigma_\infty$ , defined by (22), satisfies the metastability matrix equation. To compute  $\Sigma_\infty$ , we will solve the equation (23), rather than using (22). Assuming that  $K$  is diagonalizable,  $K = V\Lambda V^{-1}$  for some diagonal matrix  $\Lambda$ . Substituting  $K = V\Lambda V^{-1}$  in (23), left-multiplying by  $V^{-1}$  and right-multiplying by  $V^{-T}$  gives

$$\Lambda V^{-1}\Sigma_\infty V^{-T} + V^{-1}\Sigma_\infty V^{-T}\Lambda = -V^{-1}\Sigma V^{-T}.$$

Since  $\Lambda$  is diagonal, the  $i, j$ th coordinate satisfies

$$(\Lambda_{ii} + \Lambda_{jj}) \cdot (V^{-1}\Sigma_\infty V^{-T})_{ij} = (-V^{-1}\Sigma V^{-T})_{ij},$$

and therefore, letting  $J$  be the all-ones matrix,

$$\Sigma_\infty = -V \frac{V^{-1}\Sigma V^{-T}}{\Lambda J + J\Lambda} V^T, \tag{24}$$

where the division is elementwise.

We conclude that the metastable distribution  $N = N^\infty + \sqrt{n}D$  will be an  $r$ -dimensional normal distribution, with expectation equal to  $N^\infty$  (since  $E[D] = 0$ ), and covariance matrix  $n\Sigma_\infty$ .

---

<sup>4</sup>Indeed, since  $Ke^{sK} = e^{sK}K$  commute (expand  $e^{sK}$  in a Taylor series), introducing  $\Sigma_\infty$  in (22) into (23)

$$\begin{aligned} \int_0^\infty Ke^{sK}\Sigma(e^{sK})^T + e^{sK}\Sigma(K e^{sK})^T ds + \Sigma &= \int_0^\infty \frac{d}{ds} \left( e^{sK}\Sigma(e^{sK})^T \right) ds + \Sigma \\ &= -\Sigma + \Sigma = 0 \end{aligned}$$